The Astrophysical Journal, 880:82 (8pp), 2019 August 1 https://doi.org/10.3847/1538-4357/ab27bd

The Physical Origin of the Venus Low Atmosphere Chemical Gradient

Daniel Cordier[1], David A. Bonhommeau[1], Sara Port[2], Vincent Chevrier[2], Sébastien Lebonnois[3], and Fernando García-Sánchez[4]
[1] Université de Reims Champagne Ardenne, CNRS, GSMA UMR 7331, F-51097 Reims, France; daniel.cordier@univ-reims.fr
[2] Arkansas Center for Space and Planetary Sciences, University of Arkansas, Fayetteville, AR 72701, USA
[3] Laboratoire de Météorologie Dynamique (LMD/IPSL), Sorbonne Universités, UPMC Univ. Paris 06, ENS, PSL Research University, Ecole Polytechnique, Université Paris Saclay, CNRS, F-75252 Paris, France
[4] Engineering Management of Additional Recovery, Mexican Petroleum Institute. Eje Central Lázaro Cárdenas Norte 152, 07730 Mexico City, Mexico
Received 2019 March 21; revised 2019 June 4; accepted 2019 June 5; published 2019 July 29

Abstract

Venus shares many similarities with the Earth, but concomitantly, some of its features are extremely original. This is especially true for its atmosphere, where high pressures and temperatures are found at the ground level. In these conditions, carbon dioxide, the main component of Venus' atmosphere, is a supercritical fluid. The analysis of *VeGa-2* probe data has revealed the high instability of the region located in the last few kilometers above the ground level. Recent works have suggested an explanation based on the existence of a vertical gradient of molecular nitrogen abundances, around 5 ppm per meter. Our goal was then to identify which physical processes could lead to the establishment of this intriguing nitrogen gradient, in the deep atmosphere of Venus. Using an appropriate equation of state for the binary mixture CO_2–N_2 under supercritical conditions, and also molecular dynamics simulations, we have investigated the separation processes of N_2 and CO_2 in the Venusian context. Our results show that molecular diffusion is strongly inefficient, and potential phase separation is an unlikely mechanism. We have compared the quantity of CO_2 required to form the proposed gradient with what could be released by a diffuse degassing from a low volcanic activity. The needed fluxes of CO_2 are not so different from what can be measured over some terrestrial volcanic systems, suggesting a similar effect at work on Venus.

Key words: planets and satellites: atmospheres – planets and satellites: individual (Venus) – planets and satellites: surfaces – planets and satellites: tectonics

1. Introduction

Venus, sometimes considered the "sister planet" of Earth, is actually very different than what that titles implies. Essentially, Venus and the Earth share similar masses, densities, and heliocentric distances (Malcuit 2015); other features differ significantly, particularly their atmospheres. For instance, at the ground level, the air of Venus is hellish: the temperature is close to 740 K and the pressure is in the vicinity of 90 bars. Because carbon dioxide dominates the atmospheric composition, with a mole fraction around 97%, at low altitude, Venusian air is a supercritical fluid. The second most abundant atmospheric compound is molecular nitrogen, with a mole fraction of about 3%. Therefore, nitrogen is also in a supercritical state. In the phase diagram displayed in Figure 1 we have plotted carbon dioxide and nitrogen's critical points as well as the pressure (P)–temperature (T) atmospheric profile measured during the descent of the *VeGa-2* probe (Lorenz et al. 2018). Venus is not the only celestial body harboring supercritical fluids. Giant planets Jupiter and Saturn, together with brown dwarfs and some exoplanets, have regions where molecular hydrogen is in the supercritical domain (Trachenko et al. 2014). In the case of terrestrial planets, supercritical fluids could be present, but less abundant. For example, on the Earth, supercritical water has been found in some hydrothermal vents (Koschinsky et al. 2008), and its presence was also known for a long time in geothermal reservoirs (Agostinetti et al. 2017). Additionally, high density and high temperature lead to efficient dissolving and extracting abilities of supercritical fluids, allowing many industrial applications (Bolmatov et al. 2013).

Recently, the existence of a gradient of chemical composition in the Venus deep atmosphere, i.e., for layers below the altitude of ∼7000 m, has been suggested (Lebonnois & Schubert 2017). The abundance of nitrogen seems to decrease from ∼3.5% at 7000 m to zero at ground level, yielding an average gradient of about 5 ppm m^{-1}. If accepted as real, the proposed gradient may have two origins: (1) a N_2–CO_2 separation due to specific fluid features (to be identified, these can be categorized as "intrinsic" origins) and (2) phenomena related to Venus surface properties, such as the continuous release of some amount of carbon dioxide from the Venusian crust or molecular nitrogen entrapping, which can be referred to as "extrinsic" origins. As a very first attempt, we have checked that the apparent composition gradient could not simply be an effect of the compressibility of the CO_2–N_2 mixture. For this purpose, we have employed an equation of state (EoS; Duan et al. 1996) specifically developed for mixtures like CO_2–N_2, under supercritical conditions. The compressibility factor (see for instance Zucker & Biblarz 2002) Z measures the deviation of real gas compressibility from an ideal behavior, and a value around unity shows a compressibility similar to that of an ideal gas. We found that the compressibility factor Z stays around 1 in the deep atmosphere of Venus. This result, also supported by laboratory measurements (Mohagheghian et al. 2015), has already been found by Lebonnois & Schubert (2017), and we confirm it.

Although the fluid under consideration here seems to exhibit ordinary compressibility properties, in Section 2 we discuss the possibility of a separation of N_2 and CO_2, induced by gravity, and facilitated by some potential properties of our supercritical mixture. In Section 3 we discuss the role of "extrinsic effects" like crust release of carbon dioxide, before concluding on a plausible scenario.

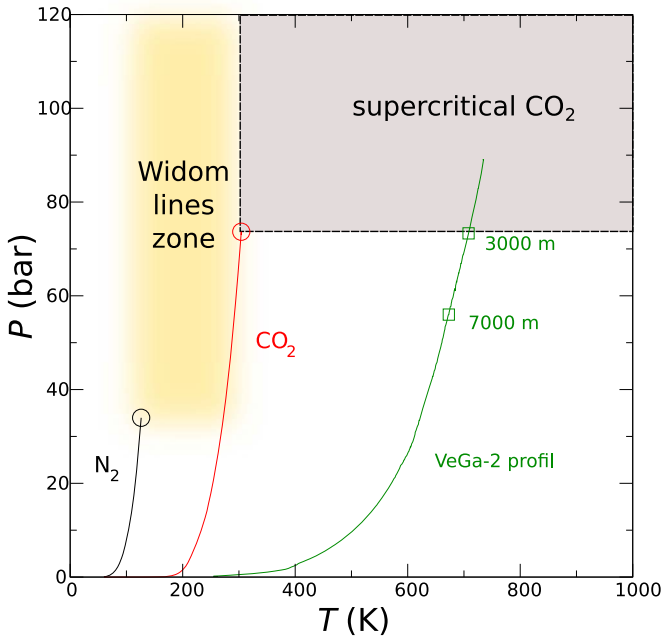

Figure 1. Simplified phase diagram of CO_2: the position of the critical point of pure CO_2 has been plotted (red circle), together with the liquid-vapor equilibrium line (red line); the supercritical CO_2 regions are shaded gray. The pressure (in bars) is denoted P, while T represents the temperature (in kelvins) of the system. Similarly, the N_2 critical point and liquid-vapor equilibrium line are shown in black. When some amount of molecular nitrogen is added to pure CO_2, the critical point of the mixture is shifted, leading to a position within the yellow-shaded zone (van Konynenburgand & Scott 1980; Goos et al. 2011). For small fractions of N_2, the position of the critical point is shifted by a few bars and a few Kelvin (Goos et al. 2011). The green line refers to the pressure–temperature profile of the Venus atmosphere derived from measurements performed by the *VeGa-2* probe (Lorenz et al. 2018).

2. The Possible Separation of N_2 and CO_2 under Supercritical Conditions

2.1. The Effect of Molecular Diffusion

For almost a century, chemical composition variations have been known among terrestrial reservoirs of hydrocarbons, i.e., containing gases or petroleum (Sage & Lacey 1939), or both. These variations are horizontal, i.e., the composition of the mixture changes from one well to another, but also vertical. In the latter case, for a given well, the abundances of species evolve with depth. The emergence of such a gradient of composition is due to the effect of gravity and to thermodiffusion. In this context, the convection is not very efficient because the fluid is trapped in a porous medium. A vast collection of literature is dedicated to this topic, and informative albeit not exhaustive reviews may be found elsewhere (Thomas 2007; Obidi 2014). Here, we focus our attention on the physics, based on molecular diffusion, of the vertical compositional grading. Our goal is to evaluate the efficiency of molecular diffusion under supercritical conditions. If the air mixing, due to atmospheric circulation, is slow or inefficient enough, the deep atmosphere of Venus could be the subject of analogous physical processes, leading to a gradient of nitrogen concentration. This assumption may also be regarded as an ideal or limiting case.

In a fluid medium undergoing a gradient of composition, temperature, or pressure, fluxes of matter appear. These transport mechanisms are ruled by the physics of irreversible physical processes. The best-known laws in this field are Fick's law of molecular diffusion and its Fourier counterpart for thermal conduction. In the general case, the total diffusion mass flux J_1 (kg m^{-2} s^{-1}) of one of the two components making a binary mixture may be written as (Bird et al. 1960; Ghorayeb & Firoozabadi 2000)

$$\boldsymbol{J}_1 = -\rho D_{12}\frac{M_1 M_2}{\bar{M}^2}\left\{\frac{\partial \ln f_1}{\partial \ln x_1}\bigg|_{P,T}\boldsymbol{\nabla} x_1 + \frac{x_1}{RT}\left(\bar{V}_1 - \frac{M_1}{\rho}\right)\boldsymbol{\nabla} P + \frac{k_{T,12}}{T}\boldsymbol{\nabla} T\right\}, \quad (1)$$

with ρ being the density (kg m^{-3}) of the mixture, D_{12} being the Fickean diffusion coefficient (m^2 s^{-1}) of species (1) in (2), M_1 and M_2 are the respective molecular weights (kg mol^{-1}) of the involved species, and $\bar{M}$ is the average molecular weight of the system: $\bar{M} = x_1 M_1 + (1 - x_1)M_2$. The fugacity, which measures non-ideal effects for a real gas, is represented by f_1 for compound (1). Adopting a typical notation, x_1 and $\bar{V}_1$ are the mole fraction of species (1) and its molar volume (m^3 mol^{-1}), and P and T are respectively the local pressure (Pa) and temperature (K). In the last term of Equation (1), the thermal diffusion ratio $k_{T,12}$ (dimensionless) is a function of $\alpha_{T,12}$, the thermal diffusion coefficient (dimensionless), according to the formula $k_{T,12} = \alpha_{T,12}\, x_1\, (1-x_1)$.

In the phenomenological Equation (1), we recognize three terms that correspond to three different processes. The first term represents the well known molecular Fickean diffusion. The second term is for pressure diffusion, which may lead to gravity segregation. The last term represents thermal diffusion (called the Soret effect for liquids), which is the tendency for species of a convection-free mixture to separate under temperature gradient.

Using the pressure and temperature gradients, provided by the *VeGa-2* probe (Lorenz et al. 2018) under steady-state conditions (i.e., $j_1 = 0$), to solve Equation (1) allows the derivation of the chemical composition as a function of altitude z. In a first approach, if we assume the Venus deep atmosphere fluid acts like an ideal gas, the equation to be integrated is simply

$$\frac{\partial x_1}{\partial z} = -\frac{x_1}{P}\left(1 - \frac{M_1}{\bar{M}}\right)\frac{\partial P}{\partial z}\bigg|_{\rm VeGa2} - \frac{\alpha_{T,12}}{T}\, x_1(1 - x_1)\frac{\partial T}{\partial z}\bigg|_{\rm VeGa2}. \quad (2)$$

In our approach, nitrogen is our chosen compound (1). We recall that, for a mixture of ideal gases, the fugacity is simply $f_1 = x_1 P$, leading to $(\partial \ln f_1/\partial \ln x_1) = 1$. The partial molar volume is, for all involved species, RT/P; and the density can be written as $\rho = P\bar{M}/RT$. Thanks to the kinetic theory of gases (Chapman & Cowling 1970), the thermal diffusion coefficient $\alpha_{T,12}$ may be estimated for the system N_2–CO_2. In the general case, $\alpha_{T,12}$ may be positive or negative, depending on the respective masses of compounds of interest. For N_2–CO_2, using Chapman & Cowling's approach, we found this coefficient to be negative. As a consequence, heavier molecules, i.e., CO_2, should gather in the coldest regions at high altitude. At the same time, the pressure term plays the opposite role, by enriching the highest layers in N_2. However,

our numerical simulations show that thermal diffusion remains notably smaller than pressure diffusion, with thermal flux around 30% of pressure flux.

By integrating Equation (2) from the top of the Venus deep atmosphere, i.e., from an altitude of 7000 m, down to the surface, we obtained a nitrogen mole fraction gradient of $\sim$0.6 ppm m^{-1}. This value is roughly one order of magnitude lower than the expected gradient (Lebonnois & Schubert 2017) of $\sim$5 ppm m^{-1}.

Now we can turn to a more realistic model; taking into account non-ideal effects, the relevant equation is then (Ghorayeb & Firoozabadi 2000)

$$\left.\frac{\partial \ln f_1}{\partial \ln x_1}\right|_{P,T}\left.\frac{\partial x_1}{\partial z}+\frac{x_1}{RT}\left(\overline{V}_1-\frac{M_1}{\rho}\right)\frac{\partial P}{\partial z}\right|_{\mathrm{VeGa2}} + \frac{\alpha_{T,12}}{T}\,x_1(1-x_1)\left.\frac{\partial T}{\partial z}\right|_{\mathrm{VeGa2}}=0. \tag{3}$$

The pressure gradient can then be expressed as a function of density and Venus' gravity g_V; we then get

$$\left.\frac{\partial \ln f_1}{\partial \ln x_1}\right|_{P,T}\frac{\partial x_1}{\partial z}=\frac{x_1}{RT}\left(\bar{V}_1-\frac{M_1}{\rho}\right)\rho\, g_V - \frac{k_{T,12}}{T}\frac{\partial T}{\partial z}. \tag{4}$$

With this new equation, we can expect the enhanced composition gradient $\partial x_1/\partial z$. Indeed, one of the criteria (Myerson & Senol 1984) used to determine the critical point position is $\partial \mu_1/\partial x_1 = 0$. This latter condition is essentially equivalent (Taylor & Krisna 1993) to $\partial\ \ln f_1/\partial\ \ln x_1 = 0$. Then, in the supercritical region, when the representative point of the system approaches the critical point, this derivative tends to zero. At the same time, the quantity $\bar{V}_1 - M_1/\rho$ generally has a non-zero finite value. As a consequence, the gradient $\partial\, x_1/\partial\, z$ could take very large values when the system is in the vicinity of the critical point. Of course, this property is unchanged if the thermodiffusion term is taken into account. In order to derive quantitative estimations we have employed the EoS (Duan et al. 1996) developed for the system CO_2–N_2 under supercritical conditions, and already used for our computations of the compressibility factor Z. The fugacity of nitrogen f_1, and its derivative, are obtained from the fugacity coefficient $\Phi_1 = f_1/P_1$ provided by the EoS. Here, the quantity P_1 denotes the partial pressure of nitrogen: $P_1 = x_1P$. The partial molar volume of N_2 comes from the equation (see the Appendix for derivation)

$$\bar{V}_1 = \frac{RT}{P}\left(1+P\left.\frac{\partial \ln \Phi_1}{\partial P}\right|_{T,x_1,x_2}\right). \tag{5}$$

We made comparisons, using the pressure–temperature profile acquired by *VeGa-2*, between quantities evaluated from the ideal gas EoS and those calculated with the help of the more advanced Duan's EoS. Not surprisingly, we found negligible differences remaining below a few percent. Concerning the derivative of the fugacity, we consistently obtained values around unity. Our simulations have shown that $\partial \ln f_1/\partial \ln x_1$ tends to zero only in the close neighborhood of the binary mixture critical point. The Venusian atmosphere seems too far from this critical point to account for the effect expected for tiny values of $\partial \ln f_1/\partial \ln x_1$, i.e., a very large gradient of chemical composition. In summary, our equilibrium model, taking into account non-ideal effects, leads to a gradient similar to the value already obtained for an ideal gas, one order of magnitude lower than what it is needed to explain the observations.

Up to this point, we have left out the question of timescales. The equilibrium states described above need a certain amount of time to be reached by the system. Since the transport processes considered in our model rely mainly on molecular diffusion, it is quite easy to make a rough estimation of the associated timescale. If H is the typical size of a system containing a fluid, the order of magnitude of the timescale τ_{diff} associated to diffusion processes is given by $\tau_{\mathrm{diff}} \sim H^2/D$ where D is the molecular diffusion coefficient. For the behavior of a solute, here nitrogen, dispersed in a volume of supercritical carbon dioxide, the value $D_{N_2-CO_2}$ (m^2 s^{-1}) of this coefficient may be evaluated with the help of the Wilke–Chang equation (Wilke & Chang 1955; Sassiat et al. 1987), which is essentially an empirical modification of the Stokes–Einstein relation

$$D_{N_2-CO_2} \simeq 7.4\times 10^{-15}\frac{TM_{CO_2}^{1/2}}{\eta_{CO_2}V_{N_2,\,b}^{0.6}}, \tag{6}$$

where T is the temperature, the molecular weight of CO_2 is M_s (44 g mol^{-1}), the viscosity of supercritical carbon dioxide is denoted η_{CO_2} (Pa s), and the molar volume of nitrogen at its boiling temperature, under atmospheric pressure, is represented by $V_{N_2,b}$. Here, we have $V_{N_2,b} \simeq 35$ cm^3 mol^{-1}. The supercritical carbon dioxide viscosity η_{CO_2} may be estimated with the help of Heidaryan et al.'s correlation (Heidaryan et al. 2011); for $T = 700$ K and $P = 100$ bar, we got $\eta_{CO_2} \sim 3\times 10^{-5}$ Pa s. All in all, we obtained $D_{N_2-CO_2} \sim 10^{-7}$ m^2 s^{-1}, a value that is roughly consistent with measurements for other simple molecules, like acetone or benzene, spread in supercritical CO_2 (Sassiat et al. 1987), for which the diffusion coefficients show values slightly above 10^{-8} m^2 s^{-1}.

In order to go beyond this first estimation, we have performed molecular dynamics (MD) simulations of CO_2–N_2 mixtures, employing the open-source package GROMACS[5,6] version 2018.2 (Abraham et al. 2015). The MD simulations have been carried out in the *NVT* ensemble (i.e., the canonical statistical ensemble) where the number of molecules N, the volume V (or equivalently the density ρ), and the temperature T of the system are constant. This ensemble has been selected for two main reasons: (i) the density of supercritical carbon dioxide, which should not significantly depart from that of the supercritical CO_2(97%)–N_2(3%) mixture, is tabulated in the NIST database at the pressures and temperatures representative of the Venusian atmosphere, unlike the isothermal compressibility that would be needed for performing MD simulations at constant pressure (*NPT* ensemble); (ii) diffusion coefficients are well defined in the *NVT* ensemble because the simulation box volume is not prone to fluctuations, and equilibrations in this thermodynamic ensemble are also less subject to numerical instabilities. The model system used for MD simulations in the

[5] GROningen MAchine for Chemical Simulations.
[6] http://www.gromacs.org

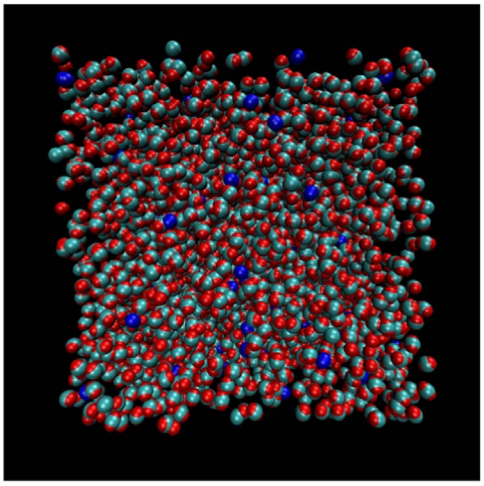

Figure 2. Supercritical fluid representing the Venusian atmosphere (97% CO_2/3% N_2) at $T = 740$ K, with $\rho = 64$kg m^{-3}. The simulation box is composed of 4850 CO_2 molecules (carbon atoms in cyan and oxygen atoms in red) and 150 N_2 molecules (nitrogen atoms in blue).

NVT ensemble includes a total of 5000 molecules: 4850 CO_2 molecules together with 150 N_2 molecules (see Figure 2), then matching the typical abundances of these molecules in the deep Venus atmosphere. In particular, the conditions relevant for two altitudes have been taken into account: 740 K (density: 64 kg m^{-3}) and 673 K (density: 44 kg m^{-3}), corresponding respectively to the ground level and an altitude of ∼7000 m. Molecular dynamics uses the principles of classical mechanics to predict not only the positions and velocities of molecules as a function of time, but also transport properties (e.g., diffusion coefficients and viscosities), structural arrangements of molecules through the computation of radial distribution functions $g(r)$, free energies, and more generally any thermodynamic or dynamic quantity available from simulations at the microscopic scale. A broad variety of MD methods exist, but in the context of the Venusian atmosphere, we focused on force-field methods where the potential energy of the system is a sum of intramolecular interactions (C–O and N–N bonds, O–C–O angles) and intermolecular, that is non-bonding, interactions (Coulomb interactions and van der Waals interactions described by Lennard–Jones potentials). The carbon dioxide intermolecular parameters (i.e., the C–C well depth ϵ_{CC}, the O–O well depth ϵ_{OO}, the C–C diameter σ_{CC}, the O–O diameter σ_{OO}, and the partial charges q_C and q_O on carbon and oxygen atoms), the C–O bond length (r^0_{CO}), and the O–C–O angle (θ^0_{OCO}), have been taken from the TraPPE force field (Potoff & Siepmann 2001). The CO_2 intramolecular force constants (k^b_{CO} for the C–O bond and k^θ_{OCO} for the O–C–O angle) have been provided by the CHARMM 27[7] force field (Bjelkmar et al. 2010). For molecular nitrogen, the intermolecular parameters (i.e., the N-N well depth ϵ_{NN} and the N–N diameter σ_{NN}) have also been taken from the TraPPE force field but the N–N bond length (r^0_{NN}) and force constant (k^b_{NN}) have been derived from the accurate analytic potential-energy curve proposed by Le Roy et al. (2006) for the ground electronic state of N_2. The partial charge q_N has been taken equal to zero since N_2 is homonuclear. The van der Waals interactions between different atoms i and j (e.g., ϵ_{CN} and σ_{CN} for Lennard–Jones interactions between one carbon atom of CO_2 and one nitrogen atom of N_2) are built from the Lorentz–Berthelot mixing rules: $\sigma_{ij} = (\sigma_{ii} + \sigma_{jj})/2$ and $\epsilon_{ij} = \sqrt{\epsilon_i \epsilon_j}$. All the force-field parameters used in this work are gathered in Table 1. The "cutoff distance" for intermolecular interactions has been set to 4.5 nm, a distance 3–4 times larger than the typical 1–1.5 nm used in conventional chemical applications, to ensure that atomic correlations that may extend to ∼1 nm are not influenced by the cutoff definition. Prior to starting MD simulations, the 5000 molecules (4850 CO_2 and 150 N_2) are randomly placed in a cubic box (edge length: $a = 17.8$ nm at $T = 740$ K and $a = 20.2$ nm at $T = 673$ K) with periodic boundary conditions to model an infinite-sized fluid. At this stage the configuration of the system is not physical due to the random atomic positions; an optimization of these positions is performed to locate the system in the vicinity of a local potential-energy minimum, with this new configuration serving as the input configuration for the subsequent *NVT* simulations. The equilibrium state is roughly reached after 50 nanoseconds using a time step of 1 femtosecond. However, equilibration is carried on during 100 additional nanoseconds for the sake of checks. The diffusion coefficients are derived from the MD simulations by computing the mean-squared displacements of molecules over a 1 nanosecond production run, printing meaningful data every 1 picosecond.

Table 1
Our Molecular Dynamics Simulation Parameters

CO_2	TraPPE
ϵ_{CC} (kJ mol^{-1})	0.22449
ϵ_{OO} (kJ mol^{-1})	0.65684
σ_{CC} (nm)	0.280
σ_{OO} (nm)	0.305
q_C	0.70
q_O	−0.35
r^0_{CO} (nm)	0.116
θ^0_{OCO} (deg)	180
	CHARMM 27
k^b_{CO} (kJ mol^{-1} nm^{-2})	784884.928
k^θ_{OCO} (kJ mol^{-1})	25104
N_2	TraPPE
ϵ_{NN} (kJ mol^{-1})	0.29932
σ_{NN} (nm)	0.331
	Additional N_2 parameters
q_N	0
r^0_{NN} (nm)	0.1097679
k^b_{NN} (kJ mol^{-1} nm^{-2})	1388996.32

Following this approach, the carbon dioxide and molecular nitrogen diffusion coefficients we obtained are respectively for ground conditions

$$D^{MD}_{CO_2}(z = 0) = 7.08 \pm 0.14 \times 10^{-7} \text{ m}^2 \text{ s}^{-1}, \quad (7)$$

$$D^{MD}_{N_2}(z = 0) = 8.97 \pm 0.64 \times 10^{-7} \text{ m}^2 \text{ s}^{-1}, \quad (8)$$

while at an altitude of ∼7000 m

$$D^{MD}_{CO_2}(z = 7000) = 10.07 \pm 0.02 \times 10^{-7} \text{ m}^2 \text{ s}^{-1}, \quad (9)$$

$$D^{MD}_{N_2}(z = 7000) = 12.20 \pm 0.29 \times 10^{-7} \text{ m}^2 \text{ s}^{-1}. \quad (10)$$

[7] https://www.charmm.org

The indicated errors are the internal statistical uncertainties of our computations. Essentially, our MD simulations lead to molecular diffusion coefficients around 10^{-6} m^2 s^{-1}, roughly one order of magnitude larger than those found with our previous crude estimation based on Equation (6). These results seem to exclude any extraordinary and unexpected behavior where the diffusion coefficient of nitrogen would have been extremely high.

Then, adopting the range 10^{-7}–10^{-6} m^2 s^{-1} and taking $H \sim 7 \times 10^3$ m, for the deep Venusian atmosphere the derived timescales are $\tau_{\rm diff} \sim 10^{13}$–$10^{14}$ s, corresponding to 1.6–16 Myr. The Global Circulation Model of the atmosphere of Venus (Lebonnois & Schubert 2017) shows a dynamical time of homogenization $\tau_{\rm dyn}$, of deep atmosphere layers, of about 20 Venus days, i.e., $\tau_{\rm dyn} \sim 2 \times 10^8$ s. The duration of the possible separation process of CO_2 and N_2 has to be much shorter than $\tau_{\rm dyn}$. Clearly, in our case, even under supercritical conditions, the diffusion of molecular nitrogen would require too much time to form a noticeable compositional gradient. In addition, we have previously shown that the gradient obtained at equilibrium cannot account for the 5 ppm m^{-1} suggested in previous works (Lebonnois & Schubert 2017). Finally, we would like to emphasize that the actual molecular diffusion coefficient $D_{12,\rm act}$, of a species (1) in a real fluid is the product of D_{12} (see also Equation (1)), the molecular diffusion coefficient in the corresponding ideal gas, by the derivative of the fugacity $\partial \ln f_1 / \partial \ln x_1$. Of course, if the latter tends to zero, then $D_{12,\rm act}$ has the same behavior. As a consequence, the time required to get the equilibrium becomes infinite. As we can see, one more time, we have an argument against a N_2–CO_2 separation, based on molecular diffusion.

2.2. Macroscopic Separation Mechanism of CO_2 and N_2

Facing the question of Venus' atmosphere chemical gradient, an alternative scenario could be the formation of CO_2-enriched droplets at some altitude, prior to their fall to the ground. Such a mechanism could easily impoverish high altitude layers in CO_2, whereas layers close to the surface could be enriched in the same compound. This possibility requires a kind of "phase transition" that could form sufficiently large droplets. This issue will be discussed momentarily, but we would like to examine first whether the timescales related to this scenario could be compatible with dynamical timescales. On the Earth, the raindrops have a typical size around 1 mm (Vollmer & Möllmann 2013). For such particles of fluid, falling under gravity, the sedimenting velocity (Pruppacher & Klett 2010) V_s is given, if we neglect the small slip-correction, by the Stokes' law

$$V_s = \frac{D_1^2 g(\rho_1 - \rho_2)}{18\eta_2}, \tag{11}$$

with being D_1 the diameter (m) of the particle, g being the gravity, ρ_1 and ρ_2 being, respectively, the density (kg m^{-3}) of the droplet and that of the "ambient medium," whose viscosity (Pa s) is called η_2. If we imagine a physical mechanism, more or less similar to a phase transition, that would separate CO_2 and N_2, we can estimate the velocity of a droplet of pure supercritical CO_2 falling through a mixture of carbon dioxide and molecular nitrogen with typical Venusian mixing ratios, i.e., containing ~3.5% of N_2. In this situation, using our dedicated equation of state (Duan et al. 1996), under typical Venusian thermodynamic conditions, i.e., $P = 100$ bar and $T = 700$ K, we found a density of 76.1 kg m^{-3} for pure supercritical CO_2, and 74.9 kg m^{-3} if 3.5% of nitrogen is added to the mixture. Concerning the viscosity, we simply took the aforementioned computed value, i.e., 3×10^{-5} Pa s (see Section 2.1). Then, adopting a particle diameter of $D_1 \sim 1$ mm, and considering a value of 8.87 m s^{-2} for the surface gravity of Venus, we found a velocity $V_s \simeq 7.4 \times 10^{-2}$ m s^{-1}. This value enables us to estimate the timescale $\tau_{\rm CO_2,set}$ of pure supercritical CO_2 settling. Fixing, as previously, the size of the deep atmosphere to $H \sim 7 \times 10^3$ m, we derived $\tau_{\rm CO_2,set} \sim 10^5$ s, corresponding to ~26 hr. The timescale $\tau_{\rm CO_2,set}$ is smaller than $\tau_{\rm dyn} \sim 2 \times 10^8$ s by several orders of magnitude. Even if the result depends on the droplet sizes, it is clearly seen that the timescale characteristic of "CO_2-enriched rains" may be compatible with the timescales imposed by CO_2/N_2 dynamical mixing. We now focus our attention on the physical mechanisms that could produce CO_2-enriched droplets. Though much research is still needed in the field of supercritical fluids, stimulated by countless industrial applications and the issue of CO_2 capture and long-term storage, a substantial assemblage of literature dealing with supercritical carbon dioxide is available. On the experimental side, Hendry et al. (2013) and Espanani et al. (2016) described laboratory experiments involving CO_2–N_2 binary mixtures under supercritical conditions. In these experiments, the fluids are introduced in a cylindrical cell with an inner height of 18 cm, the pressure is chosen between 100 and 290 bar, and the entire system is roughly at ambient temperature (Hendry et al. 2013). Starting with a bulk chemical composition of 50% CO_2–50% N_2, after a transitional regime of around 60 s the authors claim that a strong compositional gradient appears with a typical value, in mole fraction, around 400% m^{-1}. Although the mentioned laboratory conditions differ significantly from those found in the deep Venusian atmosphere, this result may suggest the existence of a fast and efficient separation process on Venus.

Unfortunately, there are several arguments questioning the reality of such a separation under the reported experimental conditions. First, we have some doubts about the way the authors stirred the mixture inside the equilibrium cell: did they use a stirring device or simply rock the cell for a time until reaching equilibrium? These procedure details are not specified in Hendry et al. (2013). Some aspects of the described experiments are clearly questionable. For instance, for a mixture with overall composition of 0.75 N_2 and 0.25 CO_2 in mole fraction, the authors report an equilibrium persistence after 140 hr (see their Figure 8), indicating that the CO_2–N_2 nonhomogeneous supercritical fluid was not returning to a homogeneous state at 238°C and 31 MPa. In fact, to our knowledge, such a phenomenon has never been found in vapor-liquid equilibrium experiments for N_2+alkane at high pressures and temperatures (García-Sánchez et al. 2007). Even more intriguing, Westman et al. (2006) and Macias Pérez (2010), who performed experiments on the N_2+CO_2 system, under conditions comparable to those described by Hendry et al. (2013), observed only one single homogeneous fluid. Finally, Lebonnois et al. (2019), who tried to reproduce Hendry et al. (2013) and

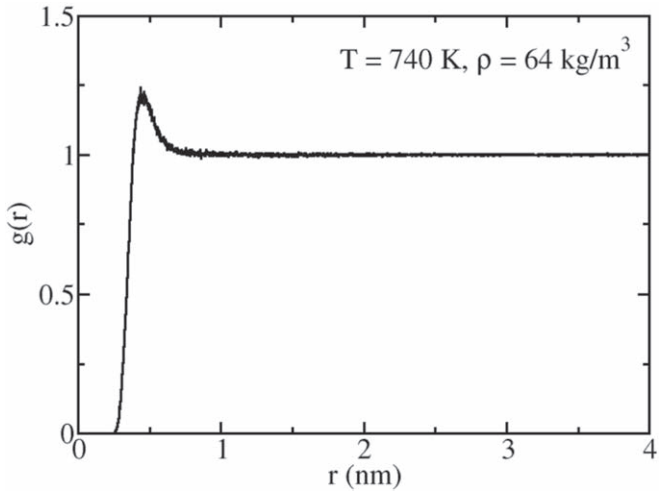

Figure 3. Radial distribution functions between CO_2 centers of mass at $T = 740$ K with $\rho = 64$kg m^{-3}. A gas-like behavior is observed: no oscillations of $g(r)$ about 1 are apparent.

Espanani et al. (2016)'s measurements, do not confirm the observations of these authors.

On the theoretical side, past works have provided evidence for the possible existence of phase separations for binary systems such as the system CO_2–N_2; nevertheless, if they exist, they must occur at high pressure (i.e., above 8×10^5 bar) and high temperature (above 2000 K) (Ree 1986). Recently, with modern molecular dynamics simulations, the concept of the "Frenkel line" has emerged for pure systems (Bolmatov et al. 2013, 2014; Brazhkin et al. 2013). This line marks, within the classical "supercritical domain," the boundary between two distinct regimes: at low-temperature, a "rigid" fluid following a liquid-like regime; and, at high-temperature, a non-rigid gas-like regime (Bolmatov et al. 2013). These new findings suggest the existence of a kind of "phase transition" when the system crosses the abovementioned "Frenkel line" (Bryk et al. 2017). Because in these works the range of pressure for the "Frenkel line" concerning the system CO_2 was not explicitly mentioned, and given that we needed computation for CO_2+N_2, we analyzed our own MD simulations, already described for the evaluation of the molecular diffusion coefficient of N_2 molecules (see Section 2.1). In Figure 3, we have plotted the radial distribution function $g(r)$ between the CO_2 center of masses for a representative numerical simulation at $T = 740$ K. Denoting A and B two CO_2 center of masses, $\langle \rho_B(r) \rangle$, the particle density of type B particles at a distance r around particles A, and $\langle \rho_B \rangle_{\rm local}$ the particle density of type B particles averaged over all the spheres of radius $a/2$ (a: length of the simulation box edge) around particles A, the radial distribution function $g_{AB}(r)$ (abbreviated to $g(r)$) writes

$$g_{AB}(r) = \frac{\langle \rho_B(r) \rangle}{\langle \rho_B \rangle_{\rm local}} = \frac{1}{\langle \rho_B \rangle_{\rm local}} \frac{1}{N_A} \sum_{i=1}^{N_A} \sum_{j=1}^{N_B} \frac{\delta(r_{ij} - r)}{4\pi r^2}. \quad (12)$$

It is a quantity aimed at evaluating the position of selected particles B with respect to a tagged particle A (CO_2 center of masses in both cases here), in order to identify the shell structure of solids (series of well-defined peaks) or gas-like behaviors ($g(r) = 1$). The shape of the curve observed in Figure 3 is characteristic of gases. We did not find any clues about the formation of CO_2 clusters, which could lead to the appearance of CO_2-enriched droplets. The simulation box view shown by Figure 2 confirms the absence of clusters. This is in agreement with our discussion of laboratory results.

Even though the field is relatively pristine, some studies investigating the properties of binary mixtures under supercritical conditions are available in the literature (Simeoni et al. 2010; Raju et al. 2017). Another demarcation within the supercritical domain is introduced, the "Widom lines," which may be multiple and delimit areas of the phase diagram where physical properties and chemical composition differ from one area to another. In Figure 1, we have indicated the phase diagram regions where the location of "Widom lines" are expected; we can see that the Vega-2 (P,T)-profile is located well outside this region.

3. Discussion and Conclusion

Given the limited likelihood for the formation of N_2 gradients due to some intrinsic properties of the N_2–CO_2 supercritical mixture, we have to turn our attention to scenarios based on extrinsic processes.

As observed by the *Magellan* mission, at the Venusian surface, volcanic features are ubiquitous (Grinspoon 2013). Although space missions did not prove the existence of an active, global volcanic cycle on Venus, another type of phenomenon may have persisted at the surface. This activity could have various indirect manifestations, among them chemical interactions between the Venusian crust and the atmosphere.

For example, nitrogen could be trapped at the surface by a geochemical process. On Earth and Mars nitrogen can be fixed via volcanism, lightning, or volcanic lightning (Segura & Navarro-Gonzalez 2005; Stern et al. 2015). The fixed nitrogen can then be trapped and accumulate on the surface under the form of nitrates or nitrites (Mancinelli 1996; Stern et al. 2015), though the stability of nitrates and nitrites on Venus remains unknown. Previous experimental studies have shown that CO_2 reacts with N_2 in the presence of electrical arcs. Thus, such a mechanism could be responsible for N_2 depletion close to the surface if lightning is significant on Venus (Tartar & Hoard 1930). There may even be a mineral on Venus that could trap or incorporate N_2 into its crystal structure, a situation sometimes seen in phyllosilicates on Earth (Mancinelli 1996; Papineau et al. 2005). The abundance of nitrogen in the surface rock is necessary to determine if one of the discussed processes could explain the absence of N_2 in the near surface atmosphere.

Under an alternative scenario, carbon dioxide could be released from the crust. As a basic assumption, we will ignore the problem of gas mixing in the atmosphere, and we assess the geological flux $F_{CO_2,\rm min}$, of CO_2 that is required to get the gradient proposed by Lebonnois & Schubert (2017). The overall picture is a certain amount of carbon dioxide substituting, molecule-by-molecule, the initial quantity of nitrogen. The latter is assumed to follow a constant profile ($x_{N_2} \sim 0.035$) from the ground to ~7000 m. According to this approach, we found $\sim 1.6 \times 10^5$ mol m^{-2} of N_2 to be replaced, leading to an average flux $F_{CO_2,\rm min} \sim 8 \times 10^{-4}$ mol m^{-2} s^{-1}, when adopting $\tau_{\rm dyn} \sim 2 \times 10^8$ s as the relevant timescale.

On the Earth, the main sources of natural carbon are volcanic. These sources can be classified into two types: direct degassing from eruptive volcanoes, and diffuse degassing from

inactive volcanoes or crustal metamorphism processes regions (Burton et al. 2013). Measuring CO_2 emission with these geophysical structures is rather challenging; accessibility and/or detectability of vents are often difficult. In addition, mixing in the atmosphere or dissolution in aquatic formations greatly complicates the task. Nonetheless, over the past few decades, the issue of climate change has motivated advances in this field. As an example, Werner & Brantley (2003) determined the CO_2 diffuse emission from the Yellowstone volcanic system: they found an average of 10^8 mol km^{-2} yr^{-1} (3×10^{-6} mol m^{-2} s^{-1}). However, this value may hide significant local variations. For instance, in the Roaring Mountain zone (see Figure 6 in Werner & Brantley 2003), the authors found a median around 10^3 g m^{-2} s^{-1} (2.7×10^{-4} mol m^{-2} s^{-1}), a value comparable to what is needed on Venus. Another diffuse source is Katla, a large subglacial volcano located in Iceland (Ilyinskaya et al. 2018). While Yellowstone measurements have been performed with the accumulation chamber method, Ilyinskaya et al. (2018) employed a high-precision airborne technique, together with an atmospheric dispersion modeling. These investigations lead to a range of 12–24 kilotons of CO_2 released per day. If brought to the surface of the glacier covering Katla, this flux corresponds to escape rates between 5.3×10^{-6} and 1.1×10^{-5} mol m^{-2} s^{-1}, values roughly one order of magnitude below what is required to sustain the Venusian atmospheric gradient. However, the total emission of CO_2 by Katla could be larger because aerial measurements may have not detected all the sources of emission, as carbon dioxide has also been found near outlet rivers by ground-based gas sensors. Finally, an overall look at known cases of volcanic systems diffusing CO_2 (Burton et al. 2013) indicates that the estimations discussed in this paragraph should be representative of the Earth's context.

Crater counting has revealed a globally youthful age for Venus' surface (Fassett 2016). The 900–1000 craters detected imply an average age between 0.2 and 1 Gyr (Korycansky & Zahnle 2005). In terms of geologic history, interpreting Venus' cratering and volcanic features is not straightforward (Fassett 2016). Two alternative scenarios can be found in the literature: (1) a catastrophic resurfacing, followed by weak activity (Schaber et al. 1992; Strom et al. 1994); and (2) a surface evolution based on a steady resurfacing, leading to a kind of equilibrium between cratering and resurfacing (Phillips et al. 1992; Bjonnes et al. 2012; Romeo 2013).

In the light of the aforementioned arguments, the chemical gradient proposed by Lebonnois & Schubert (2017) could be due to a global diffuse release of CO_2 from the crust. The flux value differences between the Earth and Venus could be explained by the different geological evolution of these planets. This argument is reinforced by the secular variability of Earth's volcanic activity over the past ~700 million years (McKenzie et al. 2016), which suggests present-day Earth entered a regime of minimum CO_2 emission. Remarkably, the suggested mechanism is compatible with both resurfacing scenarios. Together with potential thermal anomalies (Bondarenko et al. 2010; Smrekar et al. 2010; Shalygin et al. 2015), the deep atmosphere chemical gradient could be the mark of some remnant volcanic activity. The crustal average flux of CO_2 may be the "*smoking gun*" of this activity.

The problem of mixing of the CO_2 released by the crust with ambient air remains an open question. In the considered scenario, the turbulence plays a prominent role. The turbulent mixing either in the first atmospheric layers (Monin & Obukhov 1954) or in the ocean (Burchard 2002) has itself been studied for decades. Comprehensive modeling of these processes in the context of the deep Venusian atmosphere is well beyond the scope of this paper. Dedicated studies of multi-species mixing, based on laboratory experiments, have already been initiated (Bellan 2017). However, numerous works concerning mixing in turbulent jets (Dowling & Dimotakis 1990) or turbulent plumes in natural contexts (Woods 2010) are available in the literature. If a certain amount of CO_2 is locally injected into the atmosphere with a non-negligible thrust, according to the similarity found for the concentration field of gaseous turbulent jets (Dowling & Dimotakis 1990), the abundances of "fresh CO_2" should firmly decrease with altitude, possibly yielding to the proposed gradient. In all cases, the fate of this CO_2 needs further investigation because an average outgassing rate around 10^{-3} mol m^{-2} s^{-1} would lead to the doubling of the mass of the Venus atmosphere in less than 10,000 Earth years (Lebonnois et al. 2019), and neither atmospheric escape (Persson et al. 2018) nor atmospheric chemistry (Krasnopolsky 2013) seems to be able to compensate for such a flux.

For pleasure of mind, and also because the history of science is full of surprises, we cannot exclude a priori nitrogen destruction (or carbon dioxide production?) due to some very exotic "biological" activity; several authors have already explored such a scenario (Morowitz & Sagan 1967; Sagan 1967; Grinspoon 1997; Schulze-Makuch et al. 2004; Limaye et al. 2018). However, most of these works investigate hypotheses in which "life" develops in clouds, at relatively high altitude.

In the future, space probes like the pre-selected M5-mission concept *EnVision* (Ghail et al. 2012, 2017), will provide crucial data concerning Venusian geological activity, for both the surface and the near-subsurface. Indeed, *EnVision* has a proposed subsurface radar sounder that could operate to a maximum penetration depth between 250 and 1500 m under the surface of the crust (Ghail et al. 2017). This instrument appears particularly relevant for the scientific question discussed in this article.

We thank Dr. Christian Bouchot, Professor at the Instituto Politécnico Nacional (Mexico), for helpful scientific discussions. The present research was supported by the Programme National de Planétologie (PNP) of CNRS-INSU co-funded by CNES, and also partially supported by the French HPC Center ROMEO.

Appendix
Derivation of the Partial Molar Volume Equation

The partial molar volume V_i (m^3 mol^{-1}) of species i is given by (see Ghorayeb & Firoozabadi 2000, Equation (15) page 885)

$$\overline{V_i} = \left(\frac{\partial \mu_i}{\partial P}\right)_{T,\{n_j\}}, \tag{13}$$

where μ_i is the chemical potential of species i, P is the pressure, T is the temperature, and $\{n_j\}$ are the numbers of moles of the species $j \neq i$. The chemical potential for real gas mixtures may

be written as

$$\mu_i = \mu_i^0(g) + RT \ln \frac{f_i}{P_0}, \tag{14}$$

with $\mu_i^0(g)$ being the chemical potential of i in standard state, f_i being the fugacity of i, and P_0 being the reference pressure. Then the derivative is

$$\left.\frac{\partial \mu_i}{\partial P}\right|_{T,\{n_i\}} = RT \frac{\partial}{\partial P}\{\ln f_i - \ln P_0\} = RT \left.\frac{\partial \ln f_i}{\partial P}\right|_{T,\{n_i\}}. \tag{15}$$

By definition of the fugacity coefficient Φ_i we have

$$f_i = \Phi_i P_i, \tag{16}$$

where P_i is the partial pressure provided by

$$P_i = x_i P, \tag{17}$$

with x_i as the mole fraction of i and P as the total pressure. Straightforwardly,

$$\left.\frac{\partial \ln f_i}{\partial P}\right|_{T,\{n_i\}} = \left.\frac{\partial \ln \Phi_i}{\partial P}\right|_{T,\{n_i\}} + \frac{1}{P}, \tag{18}$$

leading to the desired equation

$$\bar{V}_i = \frac{RT}{P}\left\{1 + P \left.\frac{\partial \ln \Phi_i}{\partial P}\right|_{T,\{n_i\}}\right\}. \tag{19}$$

References

Abraham, M. J., Murtola, T., Schulz, R., et al. 2015, SoftX, 1-2, 19
Agostinetti, N. P., Licciardi, A., Piccinini, D., et al. 2017, Sci, 7, 14592
Bellan, J. 2017, in LPI Contributions 2061, 15th Meeting of the Venus Exploration and Analysis Group (VEXAG) (Houston, TX: Lunar and Planetary Institute), 8005
Bird, R. B., Stewart, W. E., & Lightfoot, E. N. (ed.) 1960, Transport Phenomena (New York: Wiley)
Bjelkmar, P., Larsson, P., Cuendet, M. A., Bess, B., & Lindahl, E. 2010, J. Chem. Theory Comput., 6, 459
Bjonnes, E. E., Hansen, V. L., James, B., & Swenson, J. B. 2012, Icar, 217, 451
Bolmatov, D., Brazhkin, V. V., & Trachenko, K. 2013, NatCo, 4, 2331
Bolmatov, D., Zav'yalov, D., & Zhernenkov, M. 2014, J. Phys. Chem. Lett., 5, 2785
Bondarenko, N. V., Head, J. W., & Ivanov, M. A. 2010, GeoRL, 37, L23202
Brazhkin, V. V., Fomin, Y. D., Lyapin, A. G., et al. 2013, PhRvL, 111, 145901
Bryk, T., Gorelli, F. A., Mryglod, I., et al. 2017, J. Phys. Chem. Lett., 8, 4995
Burchard, H. 2002, Applied Turbulence Modelling in Marine Waters (1st ed.; Berlin, Heidelberg: Springer)
Burton, M. R., Sawyer, G. M., & Granieri, D. 2013, RvMG, 454, 323
Chapman, S., & Cowling, T. G. 1970, The Mathematetical Theory of Non-Uniform Gases (Cambridge: Cambridge Univ. Press)
Dowling, D. R., & Dimotakis, P. E. 1990, JFM, 218, 109
Duan, Z., Møller, N., & Weare, J. H. 1996, GeCoA, 60, 1209
Espanani, R., Miller, A., Busick, A., Hendry, D., & Jacoby, W. 2016, J. CO_2 Util., 14, 67
Fassett, C. I. 2016, JGRE, 121, 1900
García-Sánchez, F., Eliosa-Jiménez, G., Silva-Oliver, G., & Godínez-Silva, A. 2007, J. Chem. Thermodynamics, 39, 893
Ghail, R., Wilson, C., Widemann, T., et al. 2017, arXiv:1703.09010
Ghail, R. C., Wilson, C., Galand, M., et al. 2012, ExA, 33, 337
Ghorayeb, K., & Firoozabadi, A. 2000, AIChE, 46, 883
Goos, E., Riedel, U., Zhao, L., & Blum, L. 2011, Energy Procedia, 4, 3778
Grinspoon, D. 2013, in Toward Understanding the Climate of Venus—Applications of Terrestrial Models to Our Sister Planet, Vol. 11 ed. L. Bengtsson et al. (New York: Springer), 266
Grinspoon, D. H. 1997, Venus Revealed: A New Look Below the Clouds of Our Mysterious Twin Planet (1st ed.; Reading, MA: Addison-Wesley)
Heidaryan, E., Hatami, T., Rahimi, M., & Moghadasi, J. 2011, J. Supercrit. Fluids, 56, 144
Hendry, D., Miller, A. W. N., Wickramathilaka, M., Espanani, R., & Jacoby, W. 2013, J. CO_2 Util., 3-4, 37
Ilyinskaya, E., Mobbs, S., Burton, R., et al. 2018, GeoRL, 45, 332, 10
Korycansky, D. G., & Zahnle, K. J. 2005, P&SS, 53, 695
Koschinsky, A., Garbe-Schönberg, D., Sander, S., et al. 2008, Geo, 36, 615
Krasnopolsky, V. A. 2013, Icar, 225, 570
Lebonnois, S., & Schubert, G. 2017, NatGe, 10, 473
Lebonnois, S., Schubert, G., Kremic, T., et al. 2019, Icar, submitted
Le Roy, R. J., Huang, Y., & Jary, C. 2006, JChPh, 125, 164310
Limaye, S. S., Mogul, R., Smith, D. J., et al. 2018, AsBio, 18, 1181
Lorenz, R. D., Crisp, D., & Huber, L. 2018, Icar, 305, 277
Macias Pérez, J. R. 2010, Master's thesis, Instituto Politécnico Nacional—Escuala Superior de Indeniería Química e Industrias Extractivas
Malcuit, R. J. 2015, The Twin Sister Planets Venus and Earth: Why are they so different? (1st ed.; Berlin: Springer)
Mancinelli, R. L. 1996, AdSpR, 18, 241
McKenzie, F. C., Horton, B. K., Loomis, S. E., et al. 2016, Sci, 352, 444
Mohagheghian, E., Bahadori, A., & James, L. A. 2015, J. Supercrit. Fluids, 101, 140
Monin, A. S., & Obukhov, A. M. 1954, TrSSR, 24, 163
Morowitz, H. A., & Sagan, C. 1967, Natur, 215, 1259
Myerson, A. S., & Senol, D. 1984, AIChE, 30, 1004
Obidi, O. C. 2014, PhD thesis, Imperial College London
Papineau, E. R., Mojzsis, S. J., & Marty, B. 2005, ChGeo, 216, 37
Persson, M., Futaana, Y., Fedorov, A., et al. 2018, GeoRL, 45, 10
Phillips, R. J., Raubertas, R. F., Arvidson, R. E., et al. 1992, JGR, 97, 15
Potoff, J. J., & Siepmann, J. I. 2001, AIChE, 47, 1676
Pruppacher, H. R., & Klett, J. D. (ed.) 2010, Microphysics of Clouds and Precipitation (Dordrecht: Reidel)
Raju, M., Banuti, D. T., Ma, P. C., & Ihme, M. 2017, NatSR, 7, 3027
Ree, F. H. 1986, JChPh, 84, 5845
Romeo, I. 2013, P&SS, 87, 157
Sagan, C. 1967, Natur, 216, 1198
Sage, B. H., & Lacey, W. N. 1939, Trans. of the AIME, 132, 143
Sassiat, P. R., Mourier, P., Gaude, M. H., & Rosset, R. H. 1987, AnaCh, 59, 1164
Schaber, G. G., Strom, R. G., Moore, H. J., et al. 1992, JGR, 97, 13
Schulze-Makuch, D., Grinspoon, D. H., Abbas, O., Irwin, L., & Bullock, M. A. 2004, AsBio, 4, 11
Segura, A., & Navarro-Gonzalez, R. 2005, GeoRL, 32, 1
Shalygin, E. V., Markiewicz, W. J., Basilevsky, A. T., et al. 2015, GeoRL, 42, 4762
Simeoni, G. G., Bryk, T., Gorelli, F. A., et al. 2010, NatPh, 6, 503
Smrekar, S. E., Stofan, E. R., Mueller, N., et al. 2010, Sci, 328, 605
Stern, J. C., Sutter, B., Freissinet, C., et al. 2015, PNAS, 112, 4245
Strom, R. G., Schaber, G. G., & Dawsow, D. D. 1994, JGR, 99, 10
Tartar, H. V., & Hoard, J. L. 1930, JAChS, 52, 156
Taylor, R., & Krisna, R. 1993, Multicomponent Mass Transfer (New York: Wiley)
Thomas, O. 2007, PhD thesis, Standford Univ.
Trachenko, K., Brazhkin, V. V., & Bolmatov, D. 2014, PhRvE, 89, 032126
van Konynenburgand, P. H., & Scott, R. L. 1980, RSPTA, 298, 495
Vollmer, M., & Möllmann, K.-P. 2013, PhTea, 51, 400
Werner, C., & Brantley, S. 2003, Icar, 4, 1061
Westman, S. F., Jacob Stang, H. G., Løvseth, S. W., et al. 2006, Fluid Phase Equilib., 409, 207
Wilke, C. R., & Chang, P. 1955, AIChE, 1, 264
Woods, A. W. 2010, AnRFM, 42, 391
Zucker, R. G., & Biblarz, O. 2002, Fundamentals of Gas Dynamics (New York: Wiley)